Case Studies in Thermal Engineering 64 (2024) 105461

Contents lists available at ScienceDirect

Case Studies in Thermal Engineering

journal homepage: www.elsevier.com/locate/csite

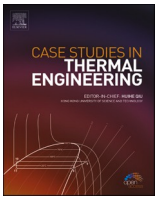

Parameters of performance: A deep dive into liquid-to-air CDU assessment

Ali Heydari [b], Ahmad R. Gharaibeh [a,*], Mohammad Tradat [b], Qusai Soud [a], Yaman Manaserh [b], Vahideh Radmard [b], Bahareh Eslami [b], Jeremy Rodriguez [b], Bahgat Sammakia [a]

[a] Department of Mechanical Engineering, ES2 Center, Binghamton University-SUNY, NY, USA
[b] NVIDIA Corp., Santa Clara, CA, USA

ARTICLE INFO

Keywords:
CDU
Heat exchanger
Liquid cooling
Data centers
Energy efficiency
Thermal management
High-power density racks
Cooling capacity
Liquid-to-air

ABSTRACT

The rapid growth in data center workloads and the increasing complexity of modern applications have led to significant contradictions between computational performance and thermal management. Traditional air-cooling systems, while widely adopted, are reaching their limits in handling the rising thermal footprints and higher rack power densities of next-generation servers, often resulting in thermal throttling and decreased efficiency, emphasizing the need for more efficient cooling solutions. Direct-to-chip liquid cooling with cold plates has emerged as a promising solution, providing efficient heat dissipation for high-performance servers. However, challenges remain, such as ensuring system stability under varying thermal loads and optimizing integration with existing infrastructure. This comprehensive study digs into the area of data center liquid cooling, providing a novel, comprehensive experimental investigation of the critical steps and tests necessary for commissioning coolant distribution units (CDUs) in direct-to-chip liquid-cooled data centers. It carefully investigates the hydraulic, thermal, and energy aspects, establishing the groundwork for Liquid-to-Air (L2A) CDU data centers. A CDU's performance was evaluated under different conditions. First, the CDU's maximum cooling capacity was evaluated and found to be as high as 89.9 kW at an approach temperature difference (ATD) of 18.3 °C with a 0.83 heat exchanger effectiveness. Then, to assess the cooling performance and stability of the CDU, a low-power test and a transient thermohydraulic test were conducted. The results showed instability in the supply fluid temperature (SFT) caused by the oscillation in fan speed at low thermal loads. Despite this, heat removal rates remained constant across varying supply air temperatures (SATs), and a partial power usage effectiveness (PPUE) of 1.042 was achieved at 100 % heat load (86 kW) under different SATs. This research sets a foundation for improving L2A CDU performance and offers practical insights for overcoming current cooling limitations in data centers.

Nomenclature

ATD	Approach temperature difference (°C)

(*continued on next page*)

* Corresponding author.
E-mail address: agharai1@binghamton.edu (A.R. Gharaibeh).

https://doi.org/10.1016/j.csite.2024.105461
Received 3 September 2024; Received in revised form 23 October 2024; Accepted 7 November 2024
Available online 8 November 2024
2214-157X/© 2024 The Authors. Published by Elsevier Ltd. This is an open access article under the CC BY license (http://creativecommons.org/licenses/by/4.0/).

(*continued*)

Nomenclature	
C	Thermal mass flow rate (kW/°C)
CC	Cooling capacity (kW)
CDU	Coolant distribution unit
CL	Cooling loop
CRAH	Computer Room Air Handler
C_p	Specific heat (kJ/kg.°C)
DC	Data center
HX	Heat exchanger
ITE	Information technology equipment
L2A	Liquid-to-air
L2L	Liquid-to-liquid
LPM	Litter per minute
P	Pressure (psi)
PG	Propylene Glycol
PPUE	Partial power usage effectiveness
Q	Volumetric flow rate (LPM)
RAT	Return air temperature (°C)
RFT	Return fluid temperature (°C)
SAT	Supply air temperature (°C)
SFT	Supply fluid temperature (°C)
T	Temperature (°C)
TTV	Thermal testing vehicle
$\dot{m}$	Mass flow rate (kg/s)
q	Heat flow rate (kW)
ε	Heat exchanger effectiveness
ρ	Fluid density (kg/m3)
ΔP	Pressure drop (psi)
ΔT_{LM}	Log mean temperature difference (°C)
Subscripts	
a	Air
in	Inlet
liq	Liquid
max	Maximum
min	Minimum
out	Outlet

1. Introduction

Data centers are the cornerstone of daily activities in today's fast-paced world, as enterprises progressively adopt cloud-based computing and incorporate Artificial Intelligence (AI) into their day-to-day operations. The ubiquity of the Internet of Things (IoT) and cryptocurrency mining leads to the widespread deployment of data centers. To satisfy the expanding demand for data processing and storage, server power density has increased, allowing additional CPUs and GPUs on a single server. That, in turn, promptly raises data center cooling demands and energy consumption, since cooling systems account for 30–50 % of overall energy usage in data centers (DCs) [1–4]. Air-cooled systems are the primary cooling form in traditional data centers, and they typically use two layouts to cool Information Technology Equipment (ITE). In the first layout, Computer Room Air Conditioner (CRAC) or Computer Room Air Handler (CRAH) units are placed in the white area around the edge of an elevated level. Via an underfloor plenum, these devices feed air, which passes through perforated tiles to the ITE. The second layout has a non-raised floor and uses peripheral units or the ceiling to supply cold air [5].

Air cooling has emerged as the predominant cooling technology in the past few years [6]. However, the restricted thermal properties of air lead to a poor convective heat transfer coefficient, which poses unique challenges for air-cooled DCs in handling the growing heat loads from high-density servers. Moreover, putting in place a successful airflow management system can be difficult as not all DCs have the resources to set it up [7–10]. Advanced cooling technologies, such as direct or indirect liquid cooling, are being incorporated independently or in tandem with conventional air-cooling solutions [11]. These technologies excel at effectively removing heat from components, a benefit attributable to fluid coolants' higher heat capacity as compared to air as a cooling medium [12–20]. The highest heat removed by conventional air-cooled data centers is usually 20–30 kW per rack. Liquid cooling, on the other hand, can raise this barrier considerably and can achieve up to 100 kW per rack [21].

Liquid cooling solutions, such as Liquid-to-Air (L2A) and Liquid-to-Liquid (L2L) systems, offer more efficient alternatives to traditional air cooling. However, implementing single-phase liquid cooling in many older data centers faces significant challenges, including the lack of raised floors, limited access to chilled water supplies, and constrained air distribution paths. To address these obstacles, L2A coolant distribution units (CDUs) have become a practical solution. L2A cooling offers a more versatile and easier-to-implement approach, particularly in legacy data centers where infrastructure limitations make L2L cooling systems impractical. Unlike L2L systems, which require extensive facility water connections and structural modifications, L2A systems can be deployed with minimal changes to existing infrastructure. This makes L2A cooling a cost-effective option for data centers looking to transition from air cooling while improving efficiency and controlling energy costs. By enhancing cooling performance without the need for major

upgrades, L2A systems provide an attractive solution for operators seeking to improve the energy efficiency of their data centers without significant capital investments.

CDUs are key elements in liquid-cooled data centers, serving a significant role in maintaining the appropriate temperatures required for the reliable functioning of servers and other essential devices, allowing denser and more compact server arrangements. CDUs are available in a variety of configurations, including in-rack, in-row, rear door, and side car [22–26]. Fig. 1 represents a general schematic for the major components of a L2A CDU. A CDU has a pump or set of pumps that circulate liquid coolant throughout the secondary loop cooling system. In the secondary loop, the liquid coolant is pumped into cooling loops that are installed on top of hot components, such as server CPUs or GPUs, where it absorbs heat. The hot fluid is then routed away from the electronic devices and toward the CDU Heat Exchanger (HX). The HX transfers heat from the fluid to the primary loop, often air by using fans to blow ambient air over the heated coolant, thereby releasing the heat into the surrounding area or by using a primary coolant such as facility water, depending on the type of HX, whether it is L2A or L2L [27,28]. Fig. 2 shows the transition from pure air cooling to hybrid cooling to fully liquid cooling.

Iyengar et al. [29] investigated hybrid cooling at the rack level, integrating air cooling for low-power equipment with liquid cooling for higher-power equipment, especially at high coolant supply temperatures. The experiments confirmed the server's capacity to handle greater coolant inlet temperatures, with water approaching 45 °C and air approaching 50 °C. Nada et al. [30] examined the thermal and hydraulic efficiency of liquid-cooled systems for servers, experimenting with alternative cooling liquid route configurations such as parallel and serpentine configurations, as well as varying geometrical dimensions, under a variety of operating conditions. Chen et al. [31] proposed employing a hybrid cooling system in addition to the primary cooling system during off-peak hours when the load on ITE hits its maximum. Shahi et al. [32] studied the effect of flow variations on the server-level cooling efficiency of a liquid cooling system. According to the study, raising the fluid flow rate has a greater impact between 0 and 50 % of the total heat load, and its relevance decreases between 50 and 100 % of the whole heat load of the server. Manaserh et al. [33] suggested an innovative approach to facilitating the construction of liquid cooling systems and evaluating the sustainability of current raised-floor data centers with limited availability of chilled water. The suggested approach entails embedding a L2A HX into perforated floor tiles, allowing the cold air provided by the unit to absorb heat from the fluid of liquid-cooled IT devices before reaching the data center space. Ling et al. [34] investigated the effects of air and cooling water input temperatures on cooling capacity in a water-cooled multi-split heat pipe system for cooling modular data center areas. The investigation showed that there was an observable increase in cooling capacity when the temperature of the cooling water decreased and the supply air temperature increased. Shahi et al. [35] characterized a row manifold for a liquid-cooled data center using liquid-to-liquid CDU, and he discovered that all of the row manifolds' ports experienced the same flow rate with a 1 lpm variance.

Heydari conducted several in-depth studies about implementing direct-to-chip liquid cooling technology using in-rack and in-row CDUs in terms of the hydraulic and thermal aspects. In terms of hydraulic aspects, Heydari et al. [36] carried out a comprehensive investigation of hydraulic transients of rack-level flow control valves under various CDU working conditions, including constant flow rate, constant differential pressure, and constant pump speed. Constant differential pressure at the CDU level was shown to be the best and the most effective, displaying superior compatibility with flow control devices and causing the smallest amount of flow rate to rise

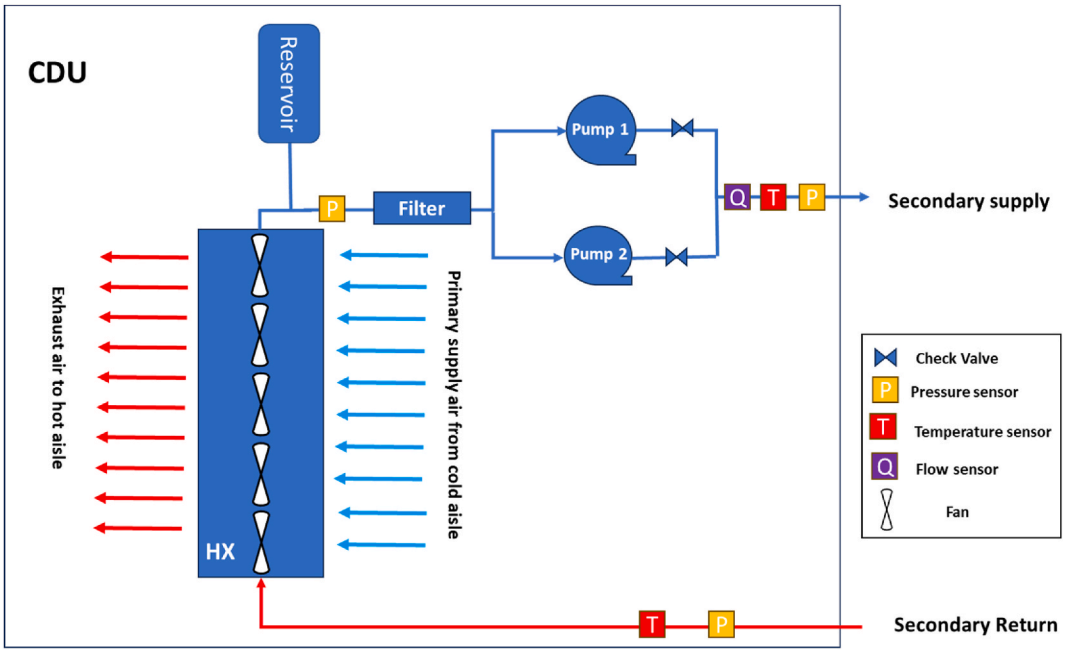

Fig. 1. Schematic diagram of the primary parts of a CDU.

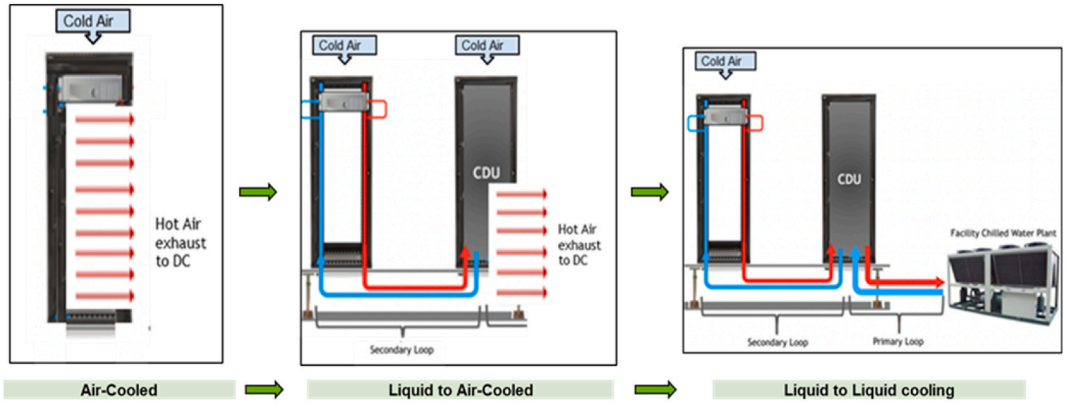

Fig. 2. Transition in cooling techniques in high power density data centers.

throughout the decommissioning of cooling loop modules located in the rack. In another study [37], he addressed general guidelines for commissioning CDUs and experimentally investigated the hydraulic performance of three different CDUs operating under various conditions, including steady-state and transient conditions. In terms of the thermal aspect, he used L2L in-rack CDU [38] to assess the effect of the temperature stability of the primary chilled water source on the overall stability of the liquid cooling system. It was shown that a minor fluctuation can translate into significant fluctuations on the secondary side if not treated promptly. Another experimental study [39] was carried out to assess the performance of rack-mountable L2A CDUs in a limited air conditioning environment. The effect of such CDUs on the room environment was presented in terms of noise generation, temperature, humidity, and air-jet speed. In a later study [40], he evaluated experimentally the performance of a L2A in-row CDU for high-heat density racks. The research looked at various thermal loads and SATs without using control or setpoints on the secondary loop temperature. He discovered that the supply fluid temperature (SFT) was affected by fan speed and thermal load, and that for 50 % heat load, the percentage of fan speed changed based on various SATs. In a recent comprehensive study on direct-to-chip liquid cooling, Heydari et al. [41] showed the adaptability of liquid cooling technology in achieving an outstanding 52 kW per rack by utilizing L2A CDUs. Furthermore, the study assessed the CDU's cooling capacity and evaluated the effectiveness of the HX. Previous studies have primarily focused on general liquid cooling systems without providing an in-depth analysis of CDU commissioning and optimization. There remains a lack of thorough experimental assessments on the critical procedures for integrating CDUs in data centers, particularly regarding performance under varying operational conditions. Addressing these gaps is essential for advancing the deployment and optimization of CDUs in modern data center environments.

This pioneering study ventures into the cutting-edge field of data center liquid cooling, offering an in-depth experimental assessment of the critical procedures and tests necessary for commissioning CDUs in direct-to-chip liquid-cooled data centers. The main goal is to build a comprehensive body of knowledge on L2A CDUs, setting a new benchmark for direct-to-chip cooling technology in data centers. This research is of high value as it directly addresses a critical gap in the deployment and optimization of liquid cooling systems, particularly in legacy data centers where infrastructure limitations restrict the use of L2L systems. By focusing on L2A HX CDUs, this study not only provides actionable insights into improving cooling capacity, HX effectiveness, and energy efficiency, but also offers a highly adaptable solution for facilities constrained by existing infrastructure. This adaptability makes L2A CDUs a crucial technology for data centers seeking to transition from traditional air cooling to more advanced, efficient cooling systems without extensive infrastructure overhauls. Moreover, the detailed assessment of key parameters—such as cooling capacity (CC), HX effectiveness, partial power usage effectiveness (PPUE), approach temperature difference (ATD), and hydraulic performance—ensures that the study contributes significantly to meeting the growing demands of high-density computing environments. As data centers continue to evolve to support advancements in AI, IoT, and cloud computing, the ability to manage increasing heat loads efficiently becomes essential. The knowledge gained from this study will have a transformative impact on the design and operation of future data centers, offering a pathway to achieving more sustainable, cost-effective, and reliable cooling solutions. These findings are crucial for enhancing operational performance, reducing energy consumption, and enabling data center operators to make informed, strategic decisions that align with long-term sustainability and operational objectives.

2. Experimental setup

The experimental setup has three racks, each of which has six thermal testing vehicles (TTVs). This configuration is designed to accommodate two in-row CDUs, as depicted in Fig. 3. The characterized CDU in this study features three pumps, six fans, and a liquid-to-air heat exchanger with a rated cooling capacity of 91 kW and a maximum fluid flow rate of 98 LPM. The CDU is equipped with centrifugal fans located at the rear of the unit within the hot aisle containment. These fans play a crucial role in optimizing the HX's performance by controlling airflow distribution and maintaining pressure across the HX. By positioning the centrifugal fans in the hot aisle containment, heated air is effectively directed away from the CDU, thus maintaining optimal thermal conditions. This setup improves the cooling capacity of the HX by facilitating better air-to-liquid heat exchange, directly impacting the overall performance of

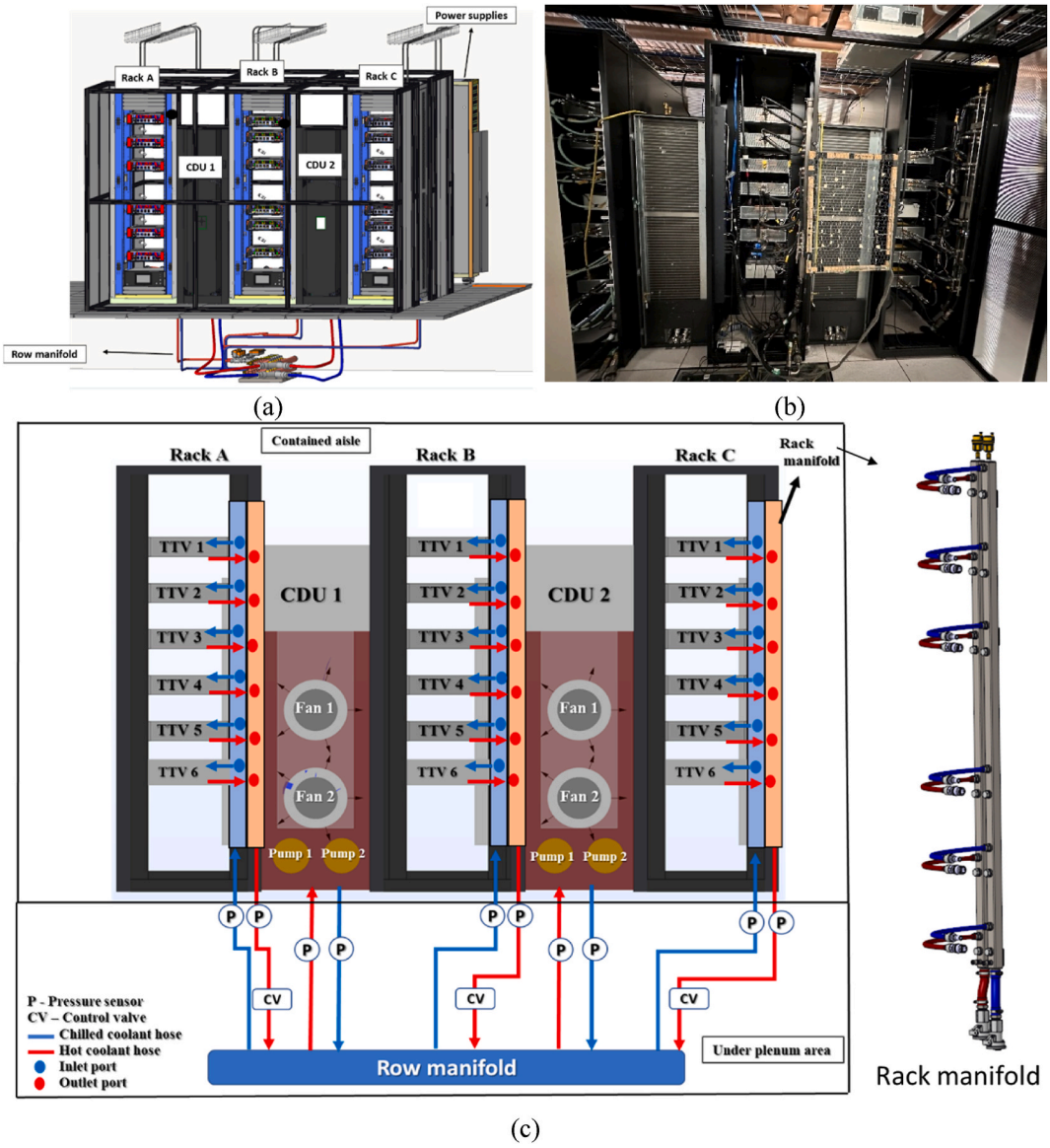

Fig. 3. The experimental setup including under plenum row manifold [40,41].

the liquid cooling system. The HX uses cold air supplied by two CRAH units through raised floor perforated tiles on the primary side by blowing air through the HX with fans and removes heat on the secondary side with PG-25, a propylene glycol and water coolant solution. Through the row manifold, the CDU feeds PG-25 to the rack manifold, which distributes the liquid to the cooling loops attached to the TTVs. Control valves are placed on the row manifold's return side for every rack. These valves are used to regulate and guarantee appropriate flow through each rack as well as to gather flow data, such as liquid temperature, glycol percentage, and liquid flow rate. Three customized rack manifold designs [26], X, Y, and Z, each having six pairs of quick disconnects, are used in this setup. The coupling between the rack manifold and the row manifold is facilitated by using FD83 coupling integral quick disconnects. The FD83 series features a turn-to-connect mechanism, which simplifies and accelerates coupling installation. This design reduces the risk of hose twisting and removes the need for extra adapters, lowering the possibility of leaks caused by faulty construction. Each rack manifold has Schrader air pocket release valves at the top that are used to remove trapped air or bubbles. This keeps excessive pressure differentials from developing, which can harm the CDU pumps.

Fig. 4 (a) is a schematic representation of the thermal testing vehicle (TTV), cooling loops, and instrumented manifold. The TTV was engineered and customized to replicate the thermal characteristics of heat-producing components [42]. The TTV comprises 14 heaters, collectively delivering a power of 9.2 kW. Among these, eight large heaters (Type X) possess a surface area of 50 mm × 50 mm, with each capable of reaching a power of 1 kW. In addition, six small heaters (Type Y) feature a surface area of 25 mm × 25 mm, each capable of generating 200 W in total power. A T-type thermocouple is installed in each heater to measure its case temperature. There

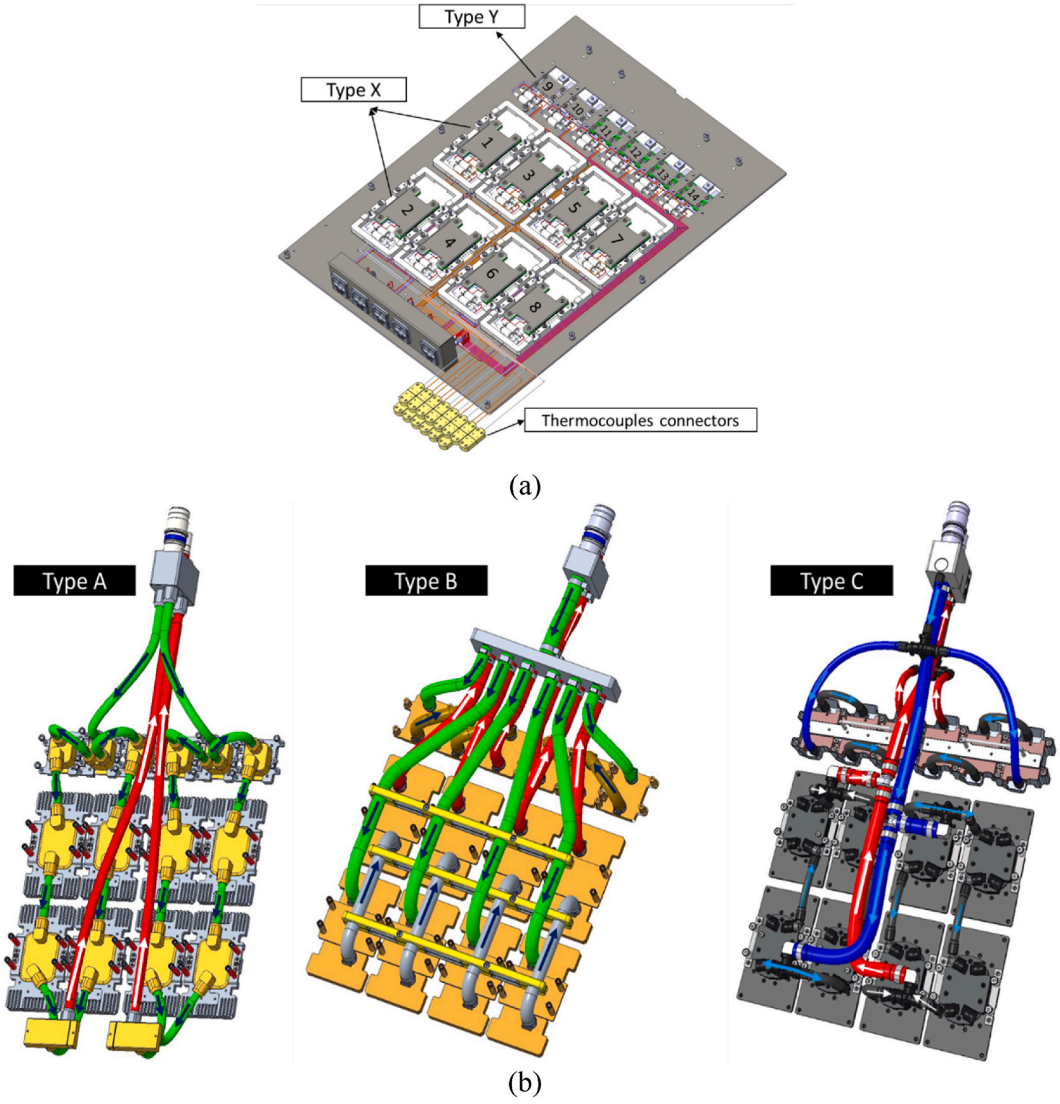

Fig. 4. (a) CAD snip for the TTVs utilized in the tests. (b) Cooling loops designs used in each rack.

are three different cooling loops deployed, as seen in Fig. 4 (b), the fluid flow inside every cooling loop is explained in Ref. [41]. Specifically, all of the TTVs in the same rack had the same cooling loops attached to them. Rack A has cooling loops A, Rack B is outfitted with cooling loops B, and Rack C is equipped with cooling loops C. Notably, each cooling loop features a unique flow distribution.

The rack manifold was connected to the cooling loops via instrumented inlet and outlet manifolds that had temperature, pressure, and ultrasonic flow meters installed. Important data, including pressure drop, cooling loop flow rate, and coolant temperatures at the inlet and exit, were all measured using this type of instrument, as shown in Fig. 5. Table 1 describes the models and specifications of the instruments utilized in the experiment.

3. Experimental procedure and evaluation stages

The first actions once a CDU arrives are conducting a visual examination and making the first article inspection (FAI) report for any damage to the internal or external parts. Following the first stages, the next step is cleaning and flushing all fittings and pipes within the CDU. Following that, critical instrumentation changes are performed to the CDU's secondary side connections to assure compliance and readiness for system connection. The starting and coolant charging stages follow, during which a thorough visual examination is performed to identify and address any possible leaks and install air-release valves at different locations to vent the trapped air in the system when starting the CDU's pumps. Several hydraulic commissioning steps must be completed after charging the CDU. This comprises looping the CDU to itself, combining the CDU with the row manifold, combining the CDU with the row manifold and rack

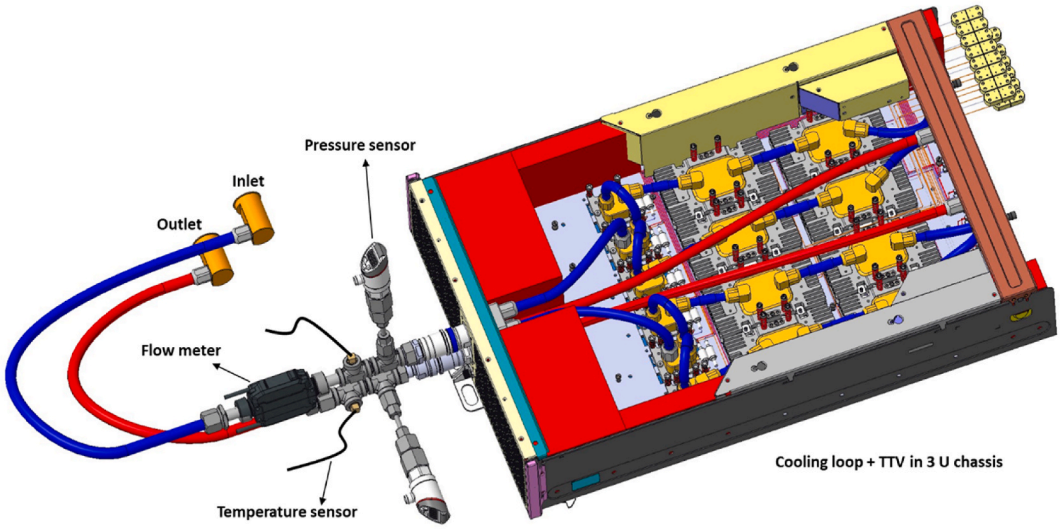

Fig. 5. The TTV heater assembly with cooling loop and instrumented manifold in 3U chassis.

Table 1
Details of the experimental instrumentation.

Items	Specification/Description	Accuracy
Airflow rate	Flow hood multimeter (ADM-850 L).	±3 % of reading
Fluid flow rate	FD-X A1 clamp-on micro flow sensor.	±0. 3 %
Air temperature	DegreeC/Cambridge AccuSense ATM2400 airflow temperature monitor.	±0.2 °C
Fluid temperature	T-type thermocouples	±0.2 °C
Heater case temperature	T-type thermocouples	±0.2 °C
Pressure sensors	KEYENCE GP-M001T (−14.50 to 14.50 PSI) KEYENCE GP-M010T (−14.5 to 145 PSI).	±1 % of full scale or less.
Power supply	Keysight PS-XHW-200	±0.1 %
IR images	FLIR E4 Thermal imaging camera with a temperature range of −20 to 250 °C.	0.15 °C thermal sensitivity
Data acquisition system	KEYSIGHT DAQ970A	–

manifolds, and lastly, integrating the CDU with the row manifold, rack manifolds, and cooling loops. Allowing this system to operate for a few hours is critical to facilitating fluid recirculation and ensuring that the CDU filters efficiently catch any contaminants inside the system. Then the unit is fully flushed and the filters visually examined. The CDU is subsequently refilled with fresh coolant to finish the hydraulic commissioning process. A flowchart demonstrating the procedures that must be performed before the actual deployment of CDU is shown in Fig. 6.

A series of tests were carried out to assess the cooling performance and stability of the CDU. Under high SAT conditions, these experiments comprised assessments at maximum and low power levels. A cooling capacity test was conducted to determine the maximum cooling capacity of the CDU and evaluate its performance under different input power levels at a fixed flow rate. Another test was carried out to investigate the effect of changing the fluid flow rate on the CDU cooling performance. Furthermore, testing was carried out within the temperature limits indicated by ASHRAE TC 9.9 from 18 °C to 27 °C [43,44]. In addition, transient thermal testing was performed to determine the CDU's stability in response to rapid changes in thermal load and fluid flow rate within the system. The following experimental procedures were implemented for the transient test.

1. Check the primary and secondary connection supplies of the CDU.
2. Connect all TTVs' cooling loops to the rack manifold.
3. Start the CDU and set the pressure that satisfies the flow rate to be supplied to the TTV cooling loops.
4. Allow enough time for the system and flow to attain stable operating conditions.
5. Apply heat load to the system gradually and wait to achieve a steady state.
6. After reaching steady-state conditions, the following sequence of events occurred:
   a. Event I: Disconnect the top TTV cable power and then disconnect the cooling loop.

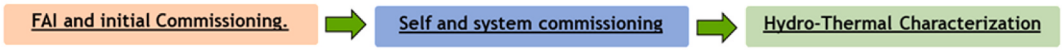

Fig. 6. The necessary stages preceding the actual deployment of CDU.

b. Event II: Disconnect the second-top TTV cable power and then disconnect the cooling loop.
c. Event III: Keep disconnecting the cable power and cooling loops until you have one cooling loop attached to the TTV in the rack.

Table 2summarizes lists of the conducted tests and the corresponding boundary conditions.

4. Performance metric

The key variables in any heat exchanger analysis are heat transfer rate (q), overall heat transfer coefficient (U), conductance curve (UA), approach temperature difference (ATD), and effectiveness (ε). The cooling capacity of the CDU HX was obtained by using Eq. (1). Where $\dot{m}_{CDU}$ is the coolant mass flow rate of the CDU, and $C_{p_{PG25}}(T)$ is the coolant specific heat as a function of fluid temperature.

$$\mathbf{q}_{CDU} = \dot{\mathbf{m}}_{CDU}\mathbf{C}_{\mathbf{p}_{\mathbf{PG25}}}\left(\mathbf{T}_{\mathbf{CDU,in}} - \mathbf{T}_{\mathbf{CDU,out}}\right) \tag{1}$$

The relationship between the heat transfer rate and the overall heat transfer coefficient times the area of heat transfer is usually plotted on a heat exchanger's conductance curve [45–48]. This is commonly written as UA and can be expressed mathematically as:

$$\textit{Thermal conductance} = \frac{q}{\Delta T_{LM}} = UA \tag{2}$$

$$\Delta T_{LM} = \frac{\Delta T_1 - \Delta T_2}{\ln\left(\frac{\Delta T_1}{\Delta T_2}\right)} \tag{3}$$

$$\Delta T_1 = RFT - RAT \tag{4}$$

$$\Delta T_2 = SFT - SAT \tag{5}$$

where ΔT_{LM} is the log mean temperature difference (LMTD) between the hot and cold fluids over the length of the heat exchanger. LMTD gives a more accurate average temperature difference for heat exchangers with large temperature variations.

The approach temperature difference (ATD) of the CDU can be calculated by subtracting the SAT from the SFT in the equation below:

$$\mathbf{ATD} = \mathbf{SFT} - \mathbf{SAT} \tag{6}$$

Another crucial metric for assessing the CDU's HX thermal performance is its effectiveness (ε). This effectiveness is expressed as the ratio of actual heat transfer to the maximum heat transfer that would take place if the fluid's temperature approached the SAT [33,41,49]. The following equation can be used to calculate the effectiveness of the HX [50]:

$$C_a = \dot{m}_a C_{p,a} \tag{7}$$

$$C_{PG25} = \dot{m}_{PG25} C_{p,PG25} \tag{8}$$

$$C_{min} = min\left(C_{PG25}, C_a\right) \tag{9}$$

$$C_{max} = max\left(C_{PG25}, C_a\right) \tag{10}$$

$$q_{max} = C_{min}\left(T_{PG25,in} - T_{air,in}\right) \tag{11}$$

$$\varepsilon = \frac{q_{CDU}}{q_{max}} \tag{12}$$

It is essential to note that while calculating the maximum possible heat transfer, the lowest value of $(\dot{\mathbf{m}}\mathbf{c}_{\mathbf{p}})$ between the fluid and air must be considered. The consideration guarantees that the top limit for heat transfer within the given conditions is accurately evaluated.

Table 2
Conducted tests and corresponding boundary conditions of the different tests.

Test	Input power (kW)	Fluid flow rate (LPM)	SAT (°C)	SFT (°C)
Maximum cooling capacity test	91.3	89	31	–
Different flow rates test	56.6	55, 80 and 94	28	–
Low power test	8.5	8.6	30	35 and 40
Transient test	51.2–8.5	48	30	45
Different SATs tests (ASHRAE recommended ranges)	86	77	19	–
	86	77	21	–
	86	77	25	–
	86	77	27	–

To determine the efficiency of certain components or subsystems in a data center rather than the overall facility, the partial power usage effectiveness (PPUE) metric is used. It quantifies a specified portion of the total PUE of a DC inside a clearly defined boundary. By focusing on a portion of the data center's infrastructure, such as a specific cooling system, power distribution unit (PDU), or IT load, PPUE provides a deeper understanding of energy efficiency. The following equation can be used to evaluate the PPUE [51]:

$$PPUE = \frac{P_{cooling} + P_{ITE}}{P_{ITE}} \tag{13}$$

where P_{ITE} is the total power used by the rack for compute, storage, and network equipment, and $P_{cooling}$ is the amount of power consumed by the CDU including pumps and fans.

5. Results

5.1. Uncertainty analysis

Uncertainty analysis is a crucial step in experimental research that evaluates and conveys the precision and reliability of the findings [52]. It examines the inherent variability and errors in every measurement to give a more thorough view of the data. The overall uncertainty is represented by Eq. (14), which takes into consideration the contributions of uncertainties related to each variable in the equation.

$$\delta_R = \sqrt{\left(\frac{\partial R}{\partial X_1}\delta_1\right)^2 + \left(\frac{\partial R}{\partial X_2}\delta_2\right)^2 + ... + \left(\frac{\partial R}{\partial X_n}\delta_n\right)^2} \tag{14}$$

In this case, the uncertainties associated with the independent variables are represented by $\delta_1, \delta_2, \ldots, \delta_n$, while the uncertainty in the final result is shown by δ_R. The measured or computed data is denoted by the variable R. This data might be dependent on other variables, such as thermal resistance, which is impacted by case temperature, coolant inlet temperature, and total power. All of the uncertainties pertaining to the observed and computed data covered in the following sections are listed in Table 3.

5.2. Hydraulic commissioning

This test considered only the hydraulic characteristics of the CDU, including pump speed, fluid flow rate, fan speed, and differential pressure. No heat load was applied to the TTVs. The CDU was operating in constant-pressure differential mode. Data were collected during the unit's commissioning stages, both when it was looped to itself and when it was incorporated into the overall system, which included the row manifold, rack manifold, and cooling loops. The CDU performed consistently, as seen in Fig. 7, with no obvious variation or instability. Furthermore, the unit functioned perfectly at the stated point, corresponding to the differential pressure setpoint.

Filtration is essential to maintaining high fluid quality, which is necessary for reliability as well as performance. It guarantees that the pipe system's solid particle levels are continuously and effectively controlled at all points. The CDU has a 75 μm filter and it was inspected at each stage of the commissioning procedure. Following the first commissioning cycle, which required looping the unit to itself, the filter caught some contaminants, as seen in Fig. 8. This emphasizes the importance of the first commissioning step in terms of promoting fluid recirculation inside the unit and properly cleaning out any debris that may be stuck in the CDU pipes during manufacturing.

5.3. Maximum cooling capacity

The maximum rated cooling capacity of the CDU was investigated by performing an experiment under specific boundary conditions. Two racks were used to achieve the desired heat load of 91.3 kW; the SAT from the CRAH units was 31 °C, and a total fluid flow rate of 89 LPM was supplied to the racks. In this test, there was no setpoint for the SFT, and the fans were running at 100 %. This configuration indicates the minimum SFT and ATD that can be achieved under those conditions. Fig. 9 shows the unit was stable in the

Table 3
Uncertainties associated with the measured and calculated parameters.

	Sensor accuracy	Uncertainty
Input power (kW)	±0.1 %	±0.1 %
Coolant flow rate (LPM)	±0. 3 %	±0.3 %
Air flow rate (m^3/s)	±3 %	±3 %
Pressure drop (°psi)	±0.145 psi	±0.2 psi
Temperature (°C)	±0.2 °C	±0.2 °C
Actual heat transfer (kW)	–	±0.15 kW
Log mean temperature difference (°C)	±0.2 °C	±0.05 °C
Thermal conductance (W/°C)	–	±30 W/°C
Effectiveness	–	±0.009
Partial power usage effectiveness	–	±0.0018

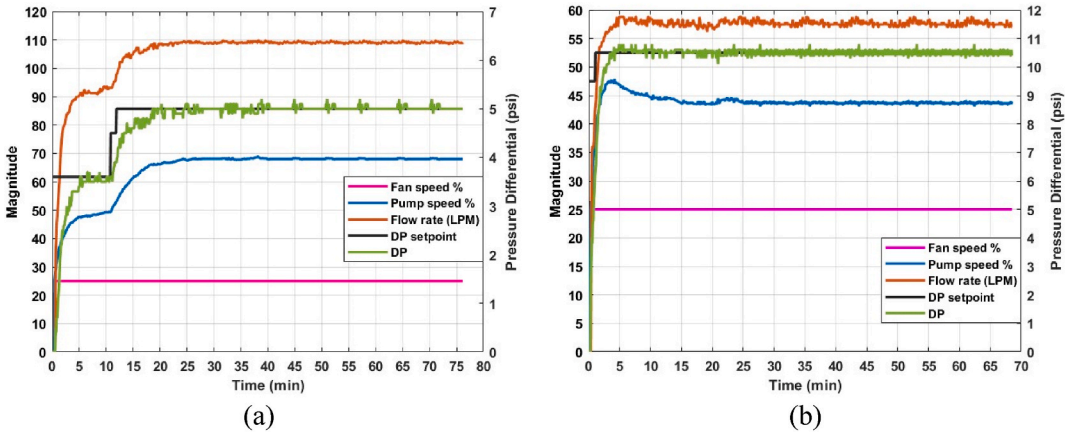

Fig. 7. CDU response parameters during commissioning when it was (a) looped to itself. (b) connected to the whole system.

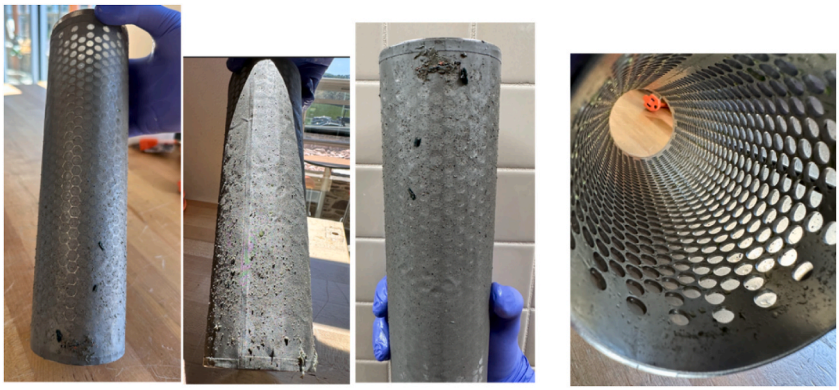

Fig. 8. Debris and other contamination caught by the filter.

thermal and hydraulic aspects, and achieved a cooling capacity (CC) of 89.9 kW at an approach temperature of 18.3 °C and 100 % fan speed. Eq. (1) was used to calculate the CDU's HX CC and from Fig. 9 (b) comparing the input power from the power supplies to the HX CC, the heat capture ratio which represents the ratio between the HX CC and the input power is around 98.5 %. The high heat capture ratio implies that thermal energy is efficiently transferred from the ITE to the cooling system. Additionally, the calculated HX effectiveness was 0.83.

5.4. Different flow rates

To investigate the effect of changing the liquid flow rate on the CDU performance and the case temperature of the TTV heaters, an experiment was carried out at three different flow rates: 55, 80, and 94 LPM, and a steady state was reached at each point. The total delivered power by the power supplies was 56.6 kW, and the SAT was 28 °C. Throughout the test, the fan speed remained fixed at 100 %, with no setpoint on the secondary fluid temperature, aiming to maximize fluid cooling and supply the lowest possible fluid temperature. Fig. 10 (a) shows that as the fluid flow rate increases, ΔT decreases as the SFT increases and the RFT decreases, decreasing from 15.1 to 8.9 °C. Generally speaking, the heat transfer coefficient increases as fluid flow rate increases. This is because increased flow rates allow the fluid's turbulence to increase, thereby improving mixing and enhancing convective heat transfer. On the other hand, a smaller ΔT occurs by greater supply fluid temperatures and lower return fluid temperatures resulting from the fluid's shorter residence time in the heat exchanger and heating sections. Fig. 10 (b) shows the HX effectiveness and ATD increased as the coolant flow rate increased while keeping the primary flow of air constant, because the increased flow enhances heat removal, improving the temperature gradient between the primary and secondary fluids. In addition, the ATD increased as SFT increased while the SAT was constant. Since the ATD is the difference between the SFT and SAT, then this leads to a larger temperature difference between the coolant and air. Fig. 10 (c) depicts the effect of fluid flow rate on the case temperature of the heaters and indicates an advantageous trend when the flow rate is increased from 55 to 80 LPM, as the corresponding case temperature shows a significant decrease of 3.5 °C. At higher flow rates, the coolant circulates more rapidly, enhancing the heat transfer between the heater and the coolant. This improved cooling efficiency keeps the heater surface cooler as heat is more quickly transferred to the coolant. However, as the flow rate increased from 80 to 94 LPM, the effect of increasing fluid flow rate decreased, as the heat transfer rate reaches a point where

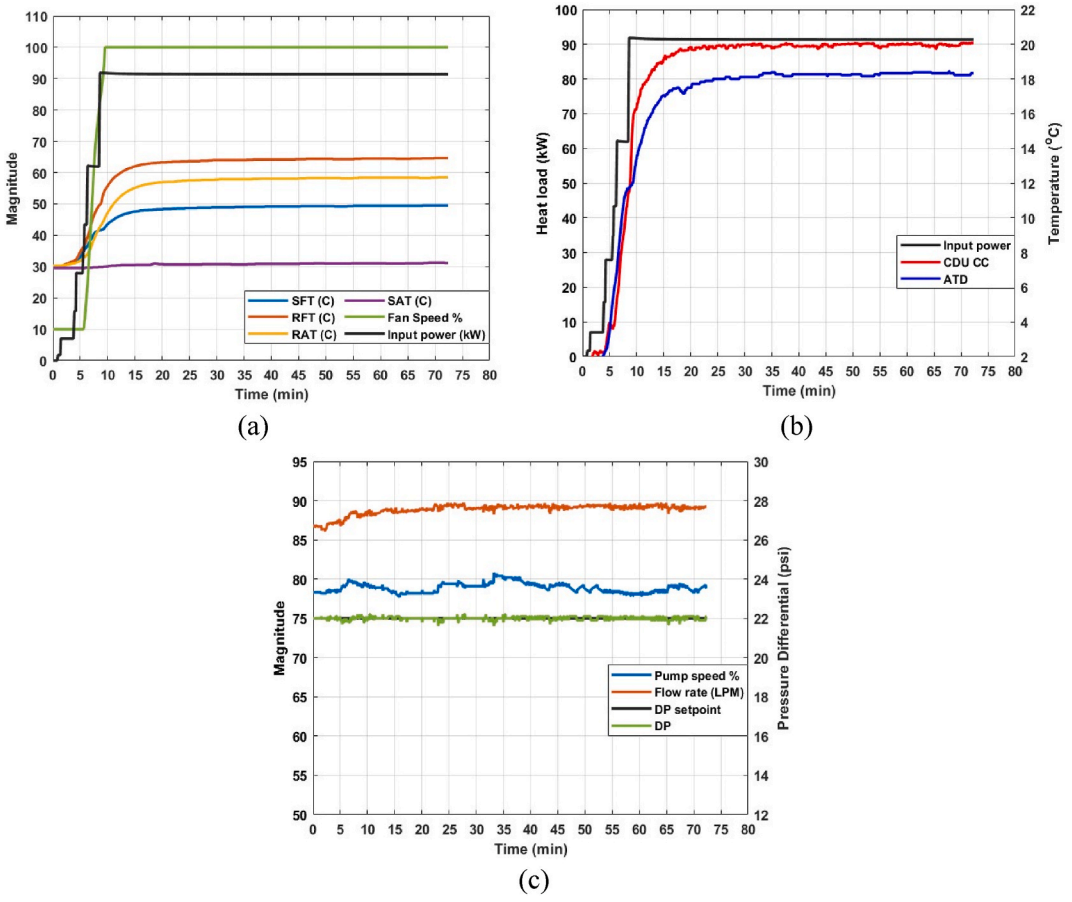

Fig. 9. Results of maximum cooling capacity test (a) CDU response parameters. (b) cooling capacity with approach temperature. (c) Hydraulic response parameters.

additional increases in flow rate have less influence on the overall cooling performance, resulting in a case temperature decrease of only 0.9 °C. A more detailed analysis is summarized in Table 4.

The effect of changing the secondary flow rate on the thermal performance of the CDU HX was examined. The conductance experimental results are shown in Fig. 11. These findings show a clear tendency of increased conductance with greater secondary flow rates. The increased conductance at higher flow rates is due to improved convective heat transfer. As the secondary fluid flow rate increases, so does the fluid's velocity and turbulence within the heat exchanger, increasing the overall heat transfer coefficient. This increased turbulence results in more efficient thermal mixing and a faster rate of heat transfer from the primary to secondary fluid. As a result, the total thermal performance of the heat exchanger increases, as demonstrated by higher conductance values. These findings are essential for enhancing the performance of L2A HX systems, especially in applications like data center cooling, where heat transfer efficiency is critical.

5.5. *Performance at low thermal duty*

The purpose of this test is to ensure that the CDU is capable of maintaining suitable cooling performance regardless of thermal duty, as well as that the temperature control and heat removal capabilities stay stable within acceptable ranges. One TTV producing 8.5 kW was used in this test; the SAT was 30 °C, and a total fluid flow rate of 8.6 LPM was supplied to the TTV. The fluid setpoint temperatures on the CDU were 35 and 40 to achieve lower ATDs of 5 and 10 °C. As seen in Fig. 12, when the desired power at the 35 °C SFT setpoint was reached, the fan speed oscillated significantly. A cascade effect of this oscillation resulted in the overshooting of the SFT, RFT, RAT, ATD, and cooling capacity. Those insights highlight the difficulties in sustaining stability in such circumstances and give insight into the CDU's instability when managing low-power devices. Therefore, the PID fan controller was modified by setting the derivative time to zero and increasing the fan integral time to stabilize the SFT on the secondary side of the loop. As shown in Fig. 12 (d), when the integral time increased, the fan speed became more stable. Nevertheless, a substantial increase in the integral time is required to effectively mitigate significant fluctuations. For the second SFT setpoint at 40 °C, the fans were running at their minimum speed to reach the setpoint temperature, and it showed more stability in the SFT, RFT, RAT, ATD, and cooling capacity as it ran at constant fan speed and achieved a cooling capacity of 7.5 kW. In terms of hydraulic performance, the pumps were running at a constant speed of

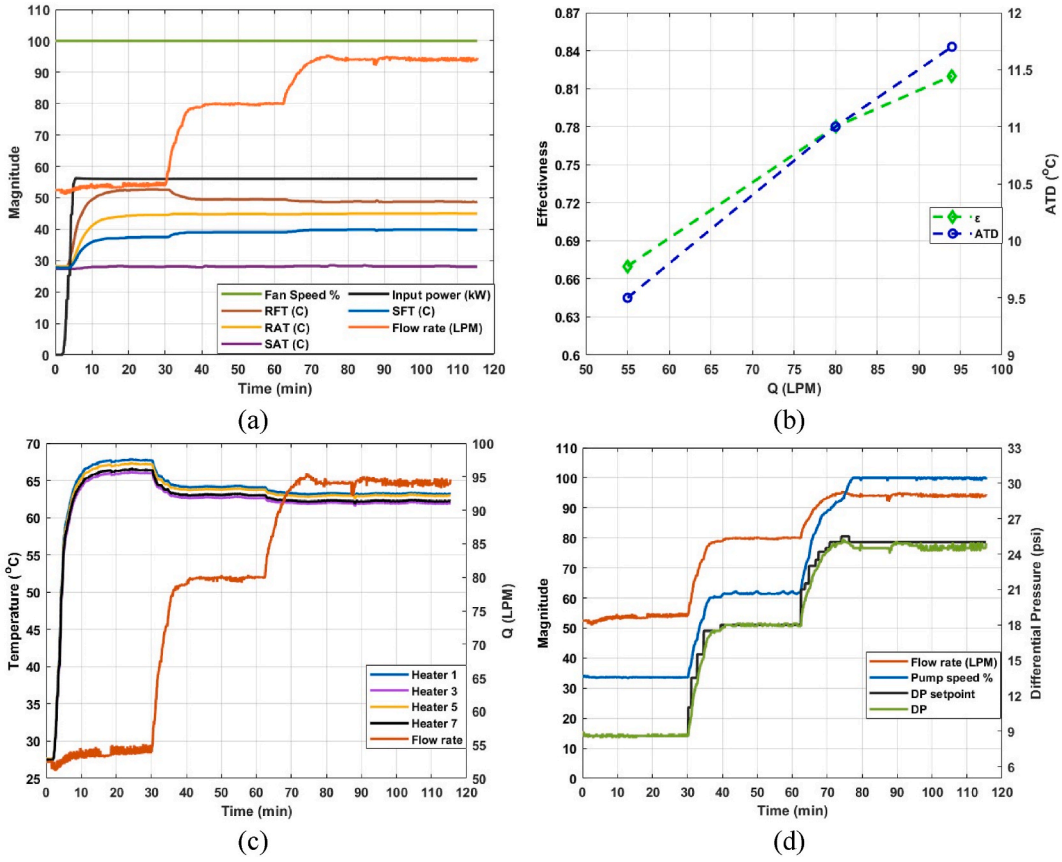

Fig. 10. Results of different fluid flow rates test (a) CDU response parameters. (b) HX effectiveness with approach temperature. (c) Heaters case temperature with flow rate. (d) Hydraulic response parameters.

Table 4
CDU response parameters for different coolant flow rates.

SAT (°C)	28	28.1	28.1
RAT (°C)	44.6	44.9	45
SFT (°C)	37.5	39.1	39.8
RFT (°C)	52.6	49.5	48.7
ATD (°C)	9.5	11	11.7
Coolant flow rate (LPM)	55	80	94
Air flow rate (CFM)	6000	5950	5960
Actual heat transfer (kW)	55.6	55.7	56
Maximum heat transfer (kW)	82.5	70.8	68.3
ε	0.67	0.78	0.82
PPUE	1.062	1.066	1.073

around 28 %, and the unit was stable and operating at the pressure setpoint of 10.5 psi, which provides the required flow rate to the TTV's cooling loop.

5.6. Transient thermohydraulic

This test determined the stability of the CDU during sudden variations in fluid flow rate and thermal load servers are connected and disconnected in multi-rack data centers. The thermal load in this test varied from the maximum rack power of 52 kW–8.5 kW by disconnecting the TTV power cords and cooling loops. The SAT was 30 °C, and a total fluid flow rate of 48 LPM, and the SFT setpoint on the CDU was 45 °C.

Fig. 13 (a) reveals that the fan speed fluctuated at every stage of disconnecting the TTVs, except when just one TTV was attached and the fans ran at their minimum speed to obtain the specified setpoint temperature of the fluid. However, because of the very low thermal load, the fans were unable to operate below 10 %, and the SFT stayed below the setpoint. Similarly, in the last test, the fan

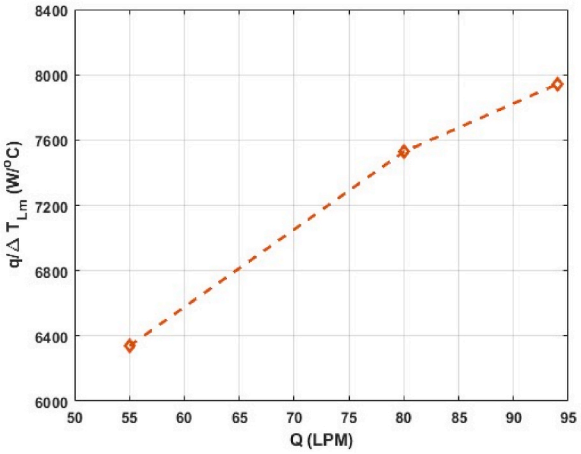

Fig. 11. HX experimental thermal conductance curve at different secondary flow rates.

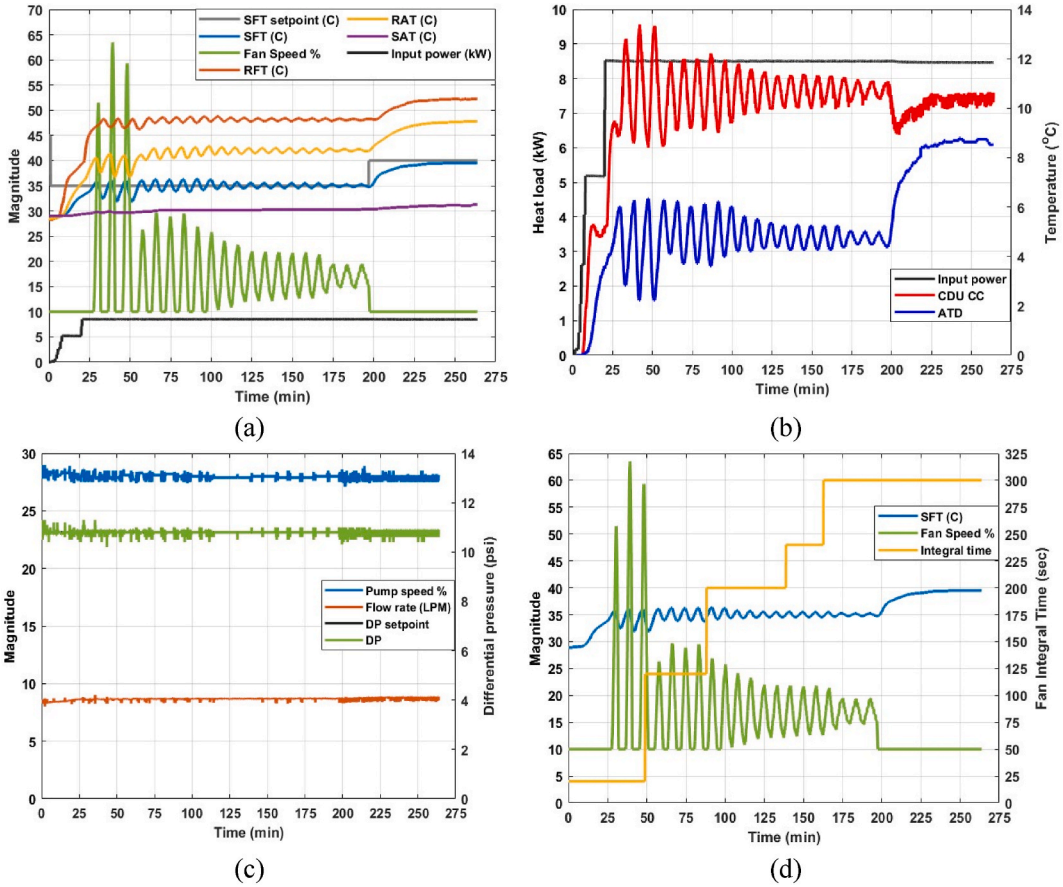

Fig. 12. Results of low power test (a) CDU response parameters. (b) cooling capacity with approach temperature. (c) Hydraulic response parameter. (d) Effect of changing PID settings on SFT and fan oscillation.

controller was adjusted by increasing the fan integral time. Nevertheless, when two TTVs were connected, even with the adjustment in fan integral time, the fan exhibited significant fluctuations. This led to instability in the SFT. Despite attempts to improve controller settings, as seen in Fig. 13 (b), the system's interaction with two TTVs remained challenging, leading to noticeable oscillations in fan speed and, therefore, the SFT. One more thing related to the oscillations in fan speed on the thermal aspect is that the CDU takes longer to achieve a steady state, as seen at each event.

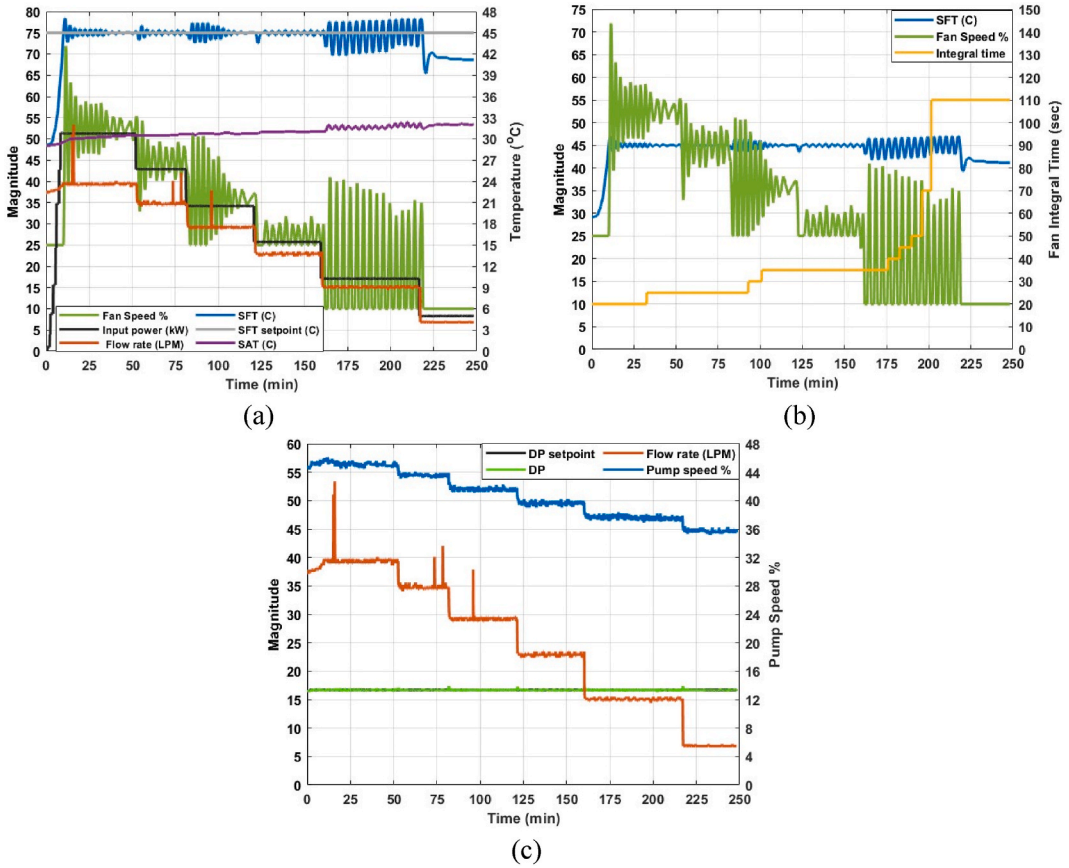

Fig. 13. Results of the transient test (a) CDU response parameters. (b) Effect of changing PID settings on SFT and fan oscillation. (c) Hydraulic response parameter.

In Fig. 13 (c), the hydraulic side of the system displayed stability without fluctuations in pressure, coolant flow rate, or pump speed, except for a jump in fluid flow rate during the initial three transient events. During each event of decommissioning the TTVs, the flow rate decreased, along with the pump speed. Overall, the unit operated satisfactorily by maintaining a constant pressure differential of 16.5 psi. This hydraulic stability, despite small changes throughout transient events, implies that the CDU efficiently managed the hydraulic parameters, maintaining steady operation and pressure stability throughout the testing periods.

5.7. ASHRAE-SAT ranges

To evaluate the CDU's performance at various SATs, four separate tests were conducted. At four different heat loads: 10 %, 50 %, 75 %, and 100 %, a steady state was reached while keeping the fluid flow rate fixed. Fig. 14 presents the outcomes of the four exams at various SATs. Fig. 14 (a) depicts the results of the 19 °C SAT test. A steady state was reached for each power level, and the SFT was around the setpoint temperature except at maximum power, where it was 1.5 °C above the setpoint. However, at 75 % heat load, the fans initially ramped up to 100 % speed but later reduced to about 80 % because the HX needed less air to maintain the setpoint fluid temperature, and the SAT dropped from 20 to 18.6 °C during that period. For the 22 and 24 °C tests as shown in Fig. 14 (b) and (c), at 10 and 50 % thermal load, the CDU achieved the SFT setpoint at different fan speeds, while it achieved a higher SFT than the setpoint when the heat load reached 75 and 100 %, although the fans were running at full speed. Another observation is on the SAT. As the heat load reached 75 %, the SAT deviated slightly from the setpoint due to minor recirculation. Fig. 14 (d) shows the results of the 27 °C test. The CDU was able to achieve the desired SFT setpoint at 10 % heat load, but the difference between the other tests was that the fan speed was not constant at 30 %; it was varying to maintain the same coolant temperature, and as the heat load increased, the fan speed jumped to 100 % for the rest of the experiment. As the heat load increased, the CDU was unable to achieve the same SFT setpoint, and it was above the setpoint to maintain the appropriate ATD that could remove the heat load.

A summary of the CDU data at maximum input power is shown in Table 5. The results demonstrate that the unit maintains a similar amount of cooling capacity and effectiveness across varying SATs because they have the same ATD. However, with a 22 °C SAT, the ATD varies because of a decreased air mass flow rate entering the HX, leading to a higher SFT. Additionally, the heat removed by the CDU HX was divided by the total input power supplied by the power sources to estimate the coolant's average heat capture ratio. 94 % of the heat was captured, according to the study's results.

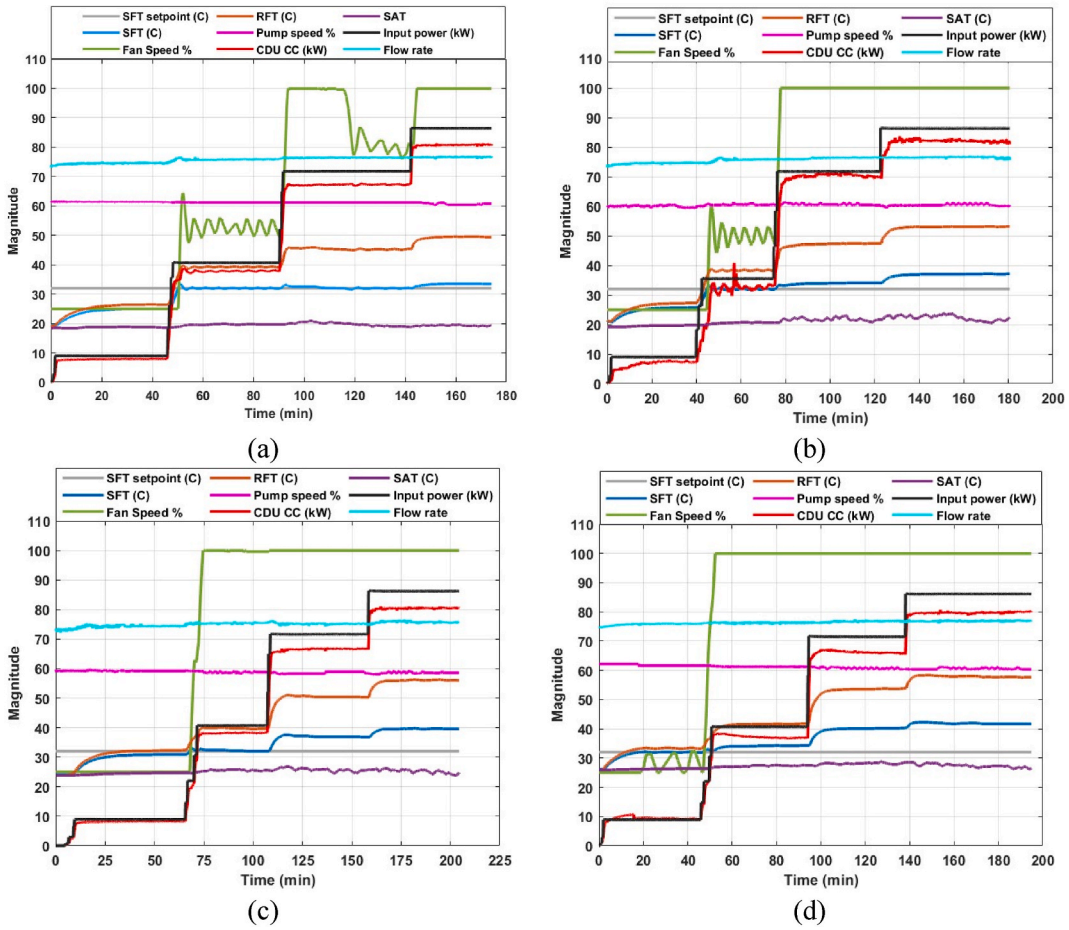

Fig. 14. Test results of (a) 19 °C SAT. (b) 22 °C SAT. (c) 25 °C SAT. (d) 27 °C SAT.

Table 5
CDU response parameters.

Test	19 °C	22 °C	25 °C	27 °C
SAT (°C)	19	22	25	27.2
RAT (°C)	42.3	45.6	48.7	50.7
SFT (°C)	33.5	37	39.5	41.6
RFT (°C)	49.5	53.1	56	57.7
ATD (°C)	14.5	15	14.5	14.4
Coolant flow rate (LPM)	77	77	77	77
Air flow rate (CFM)	5538	5405	5687	5750
Actual heat transfer (kW)	80.9	80.5	79.8	80.4
Maximum heat transfer (kW)	98.6	96.9	97.3	96.8
ε	0.82	0.83	0.82	0.83

5.8. PPUE analysis

PPUE accounts for all infrastructure components and serves as an energy consumption metric within established boundaries, dividing the data center into zones. In our analysis, we took into account the power consumption of the CDU and TTVs in the liquid-cooled racks. Fig. 15 (a) demonstrates that the PPUE dropped by 5 % as the heat load increased from 10 % to 100 %, with the pumping power kept constant by maintaining a fixed flow rate. The increase in heat load resulted in improved cooling system efficiency, due to a more favorable ratio of heat removed to power consumed. This suggests that the data center's infrastructure becomes more energy-efficient as the heat load increases. This might be because greater loads make better use of the cooling capacity and other infrastructure components. On the other hand,Fig. 15 (b) shows that when the flow rate increased, the PPUE went up. The increased power usage of the cooling system's pumps is the reason for this, since their speed climbed from 33 % to 100 % at the maximum secondary flow. Fig. 15 (C) indicates that the SAT at minimum and maximum heat loads appears to have no impact on the PPUE since the cooling

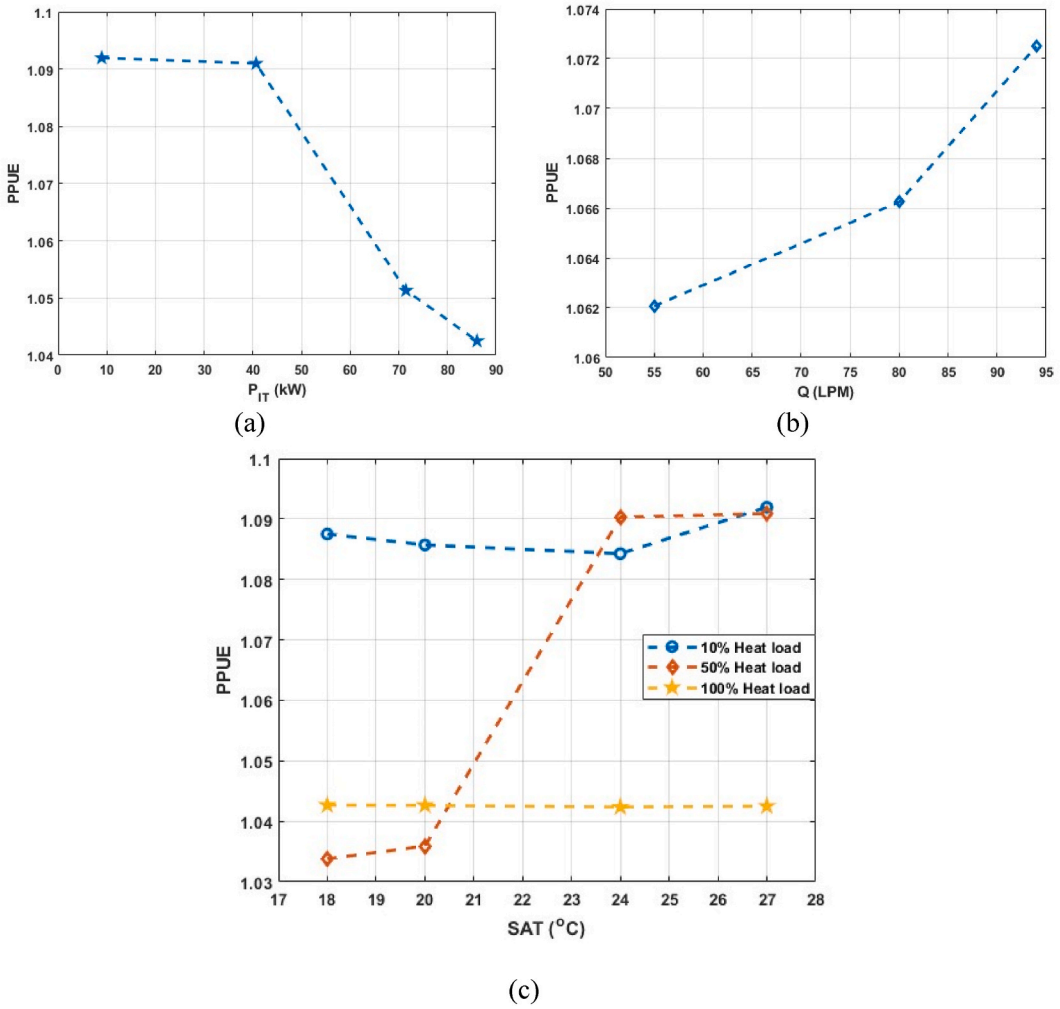

Fig. 15. PPUE calculated values at (a) Different heat loads. (b) Different fluid flow rates. (c) Different SATs.

system's power consumption at the same heat load is nearly identical. However, with a 50 % heat load, the PPUE changes and increases at SATs of 24 °C and 27 °C as the fan speed increases, eventually reaching 100 %. This indicates that running the ITE at maximum heat load demonstrates an effective and well-designed cooling system capable of maintaining consistent energy consumption despite changes in SAT.

5.9. Challenges and solutions

One significant challenge encountered during the commissioning process for CDUs is in the thermal commissioning phase. This involves addressing fluctuations in fan speed, which can cause instability in SFT. Such instabilities can influence the CDU cooling capacity, HX effectiveness, and TTV heater case temperatures. To overcome that issue, the fans' PID configurations must be changed—either manually or with the use of an adaptive PID controller. The adaptive PID controller provides a way to reduce fan speed oscillations during thermal commissioning by dynamically choosing the proper PID settings for different circumstances. An additional point to consider about the fan speed fluctuations is that the CDU takes a longer time to achieve a steady state. This implies that before the system settles into a stable operating state, it goes through an extended transient period. The longer time to establish a steady state can indicate complicated interactions and thermal dynamics inside the entire system, necessitating additional research and appropriate modifications to the control method to improve thermal performance and decrease transient response time.

Another issue might come up during thermal commissioning, which is the recirculation of the hot air between the hot and cold aisle containment. This issue can be effectively solved by installing blanking panels on the back of the racks, as proposed in Ref. [41]. Fig. 16 demonstrates the effective elimination of the air recirculation issue through the use of blanking panels.

(a) (b) (c)

Fig. 16. IR images for the back of the rack (a) without blanking panels. (b) and (c) with blanking panels.

6. Conclusion

A major objective of the current study was to develop a comprehensive understanding of liquid-to-air CDUs for direct-to-chip cooling in data centers, with a primary focus on achieving the highest possible energy efficiency and enhancing thermal performance compared to conventional air cooling. This study intends to create a solid framework for their implementation and assessment, enabling long-term effective integration. Based on the detailed analysis of the experimental commissioning and testing results, the following conclusions can be drawn.

- It is imperative that the secondary loop circuit be flushed prior to connecting the CDU to the liquid cooling lines that transfer coolant from or to the cold plates, such as row and rack manifolds.
- Approximately 90 kW of cooling capacity was reported at an approach temperature of 18.3 °C and a secondary coolant flow rate of 89 LPM.
- A heat exchanger's cooling capacity and effectiveness are independent of the supply air temperature and are strongly affected by the approach temperature and the flow rate of the secondary coolant.
- It was challenging to maintain a stable supply coolant temperature at low thermal loads, and this affected the heat exchanger's cooling capacity and, consequently, its effectiveness as a result of fluctuations in fan speed.
- To overcome the fluctuations in fan speed, PID control must be adjusted.
- The implementation of an adaptive PID controller stabilized fan speed, and at the 40 °C setpoint, the cooling system achieved 7.5 kW of cooling capacity with more consistent fluid temperature regulation.
- In the transient test, thermal loads varied from 52 kW to 8.5 kW, causing fluctuations in fan speed and supply fluid temperature. Despite this, the hydraulic system maintained a steady pressure differential of 16.5 psi, demonstrating the CDU's stability under sudden load and flow changes.
- The cooling system is resilient and efficient at both ends of the heat load spectrum. However, higher SATs at mid-loads can result in increased power consumption due to higher fan speeds.
- To adopt an increase in the power density per rack, the following steps should be taken:
  - o Achieve higher cooling capacities at lower ATDs.
  - o Implement an adaptive PID controller to achieve smoother fan operation during fluctuations in thermal load.
  - o To improve the cooling capabilities of the CDU and the efficiency of the heat exchanger, an improved pumping curve is essential.

CRediT authorship contribution statement

Ali Heydari: Writing – review & editing, Supervision, Project administration, Methodology. **Ahmad R. Gharaibeh:** Writing – review & editing, Writing – original draft, Visualization, Validation, Supervision, Software, Resources, Methodology, Investigation, Formal analysis, Data curation, Conceptualization. **Mohammad Tradat:** Writing – review & editing, Supervision, Project administration, Methodology, Conceptualization. **Qusai Soud:** Writing – review & editing, Investigation. **Yaman Manaserh:** Writing – review & editing, Visualization, Supervision, Methodology. **Vahideh Radmard:** Writing – review & editing. **Bahareh Eslami:** Writing – review & editing. **Jeremy Rodriguez:** Writing – review & editing, Project administration, Funding acquisition. **Bahgat Sammakia:** Writing – review & editing, Supervision, Project administration, Methodology, Funding acquisition, Conceptualization.

Declaration of competing interest

The authors declare that they have no known competing financial interests or personal relationships that could have appeared to influence the work reported in this paper.

Acknowledgment

We would like to acknowledge NVIDIA. This work is supported by NVIDIA and NSF IUCRC Award No. IIIP-2209776 and MRI Award No. CNS1040666.

Data availability

The data that has been used is confidential.

References

[1] Y. Ma, G. Ma, S. Zhang, S. Xu, Experimental investigation on a novel integrated system of vapor compression and pump-driven two phase loop for energy saving in data centers cooling, Energy Convers. Manag. 106 (Dec. 2015) 194–200, https://doi.org/10.1016/J.ENCONMAN.2015.09.004.
[2] X. Wang, et al., Energy, exergy, and economic analysis of a data center energy system driven by the CO2 ground source heat pump: prosumer perspective, Energy Convers. Manag. 232 (Mar. 2021) 113877, https://doi.org/10.1016/J.ENCONMAN.2021.113877.
[3] X. Qian, Z. Li, Z. Li, A thermal environmental analysis method for data centers, Int. J. Heat Mass Tran. 62 (1) (Jul. 2013) 579–585, https://doi.org/10.1016/J.IJHEATMASSTRANSFER.2013.03.037.
[4] S. Nada, R. El-Zoheiry, M. E.-C. S. in T, and undefined, Experimental investigation of hydrothermal characteristics of data center servers' liquid cooling system for different flow configurations and geometric. ElsevierSA Nada, RM El-Zoheiry, M Elsharnoby, OS OsmanCase Studies in Thermal Engineering, 2021•Elsevier, 2021. https://www.sciencedirect.com/science/article/pii/S2214157X21004391. (Accessed 2 September 2024).
[5] V.S. Simon, H. M.-I., and undefined, Feasibility study of rear door heat exchanger for a high capacity data center, asmedigitalcollection.asme.org, 2022, in: https://asmedigitalcollection.asme.org/InterPACK/proceedings-abstract/InterPACK2022/V001T01A018/1153380?casa_token=BqdCvJnmy0wAAAAA:1ZQuZJlB1w73v6So_T93OPwlt_HaHCLa8waYpeWzGTgnuRDLt6RTFbdpyGniaJDUcjs4ofpaXw. (Accessed 4 December 2023).
[6] M. Romero-Lara, F. Comino, M. de A.-E. C. and, and undefined, Experimental assessment of the energy performance of a renewable air-cooling unit based on a dew-point indirect evaporative cooler and a desiccant wheel. ElsevierMJ Romero-Lara, F Comino, MR de AdanaEnergy Conversion and Management, 2024•Elsevier, 2024. https://www.sciencedirect.com/science/article/pii/S0196890424004278. (Accessed 5 June 2024).
[7] S. Kadam, R.K. I, J. of T. Sciences, and undefined, Twenty First Century Cooling Solution: Microchannel Heat Sinks, Elsevier, 2014. https://www.sciencedirect.com/science/article/pii/S129007291400163X?casa_token=1wbE4brXT-4AAAAA:7QgmBX4aNXy_9o0EwZ2foiPsj1ic5NISwBzALA7zIzlyPNgF84HlXvsPRDD2b15DuAg90M3sOxpD. (Accessed 14 April 2023).
[8] I. Sauciuc, G. Chrysler, R. Mahajan, M. Szleper, Air-cooling extension - performance limits for processor cooling applications. Annual IEEE Semiconductor Thermal Measurement and Management Symposium, 2003, pp. 74–81, https://doi.org/10.1109/STHERM.2003.1194342.
[9] J. Dai, M.M. Ohadi, D. Das, M.G. Pecht, Optimum cooling of data centers: application of risk assessment and mitigation techniques. Optimum Cooling of Data Centers: Application of Risk Assessment and Mitigation Techniques, Jan. 2014, pp. 1–186, https://doi.org/10.1007/978-1-4614-5602-5/COVER.
[10] E. Oró, A. Garcia, J. S.-E. and Buildings, and undefined, Experimental and Numerical Analysis of the Air Management in a Data Centre in Spain, Elsevier, 2016. https://www.sciencedirect.com/science/article/pii/S0378778816300366. (Accessed 14 April 2023).
[11] G.D. Chethana, B.S. Gowda, Thermal management of air and liquid cooled data centres: a review, Mater Today Proc 45 (Jan. 2021) 145–149, https://doi.org/10.1016/J.MATPR.2020.10.396.
[12] A.C. Kheirabadi, D. Groulx, Experimental evaluation of a thermal contact liquid cooling system for server electronics, Appl. Therm. Eng. 129 (Jan. 2018) 1010–1025, https://doi.org/10.1016/J.APPLTHERMALENG.2017.10.098.
[13] R. Schmidt, M. Steinke, A. S.-A. Journal, and undefined, Moderating the Impact of Integrating Water-Cooled Servers into Data Centers, airah.org.au, 2019. https://www.airah.org.au/Content_Files/EcoLibrium/2021/10-21-Eco-technical-paper.pdf. (Accessed 2 December 2022).
[14] A.R. Gharaibeh, Y.M. Manaserh, M.I. Tradat, F.W. AlShatnawi, S.N. Schiffres, B.G. Sammakia, Using a multi-inlet/outlet manifold to improve heat transfer and flow distribution of a pin fin heat sink, J. Electron. Packag. 144 (3) (Sep. 2022), https://doi.org/10.1115/1.4054461.
[15] C.H. Hoang, et al., Impact of fin geometry and surface roughness on performance of an impingement two-phase cooling heat sink, Appl. Therm. Eng. 198 (Nov. 2021) 117453, https://doi.org/10.1016/J.APPLTHERMALENG.2021.117453.
[16] A. Carbó, E. Oró, J. Salom, M. Canuto, M. Macías, J. Guitart, Experimental and numerical analysis for potential heat reuse in liquid cooled data centres, Energy Convers. Manag. 112 (Mar. 2016) 135–145, https://doi.org/10.1016/J.ENCONMAN.2016.01.003.
[17] H. Wang, et al., Performance evaluation and optimization of data center servers using single-phase immersion cooling, Int. J. Heat Mass Tran. 221 (Apr. 2024) 125057, https://doi.org/10.1016/J.IJHEATMASSTRANSFER.2023.125057.
[18] Y.A. Manaserh, A.R. Gharaibeh, M.I. Tradat, S. Rangarajan, B.G. Sammakia, H.A. Alissa, Multi-objective optimization of 3D printed liquid cooled heat sink with guide vanes for targeting hotspots in high heat flux electronics, Int. J. Heat Mass Tran. (Dec. 2021) 122287, https://doi.org/10.1016/J.IJHEATMASSTRANSFER.2021.122287.
[19] M. Hnayno, A. Chehade, H. Klaba, G. P.-C. S. in T, and undefined, Experimental investigation of a data-centre cooling system using a new single-phase immersion/liquid technique. ElsevierM Hnayno, A Chehade, H Klaba, G Polidori, C MaaloufCase Studies in Thermal Engineering, 2023•Elsevier, 2023. https://www.sciencedirect.com/science/article/pii/S2214157X23002319. (Accessed 2 September 2024).

[20] F. Naduvilakath-Mohammed, R. J.-C. S. in T, and undefined, Closed loop liquid cooling of high-powered CPUs: a case study on cooling performance and energy optimization. ElsevierFM Naduvilakath-Mohammed, R Jenkins, G Byrne, AJ RobinsonCase Studies in Thermal Engineering, 2023•Elsevier, 2023. https://www.sciencedirect.com/science/article/pii/S2214157X23007785. (Accessed 2 September 2024).

[21] K.W. Yan, P.Y. Lin, S.L. Kuo, Thermal challenges for HPC 3DFabricTMPackages and systems, in: IEEE International Reliability Physics Symposium Proceedings, 2022-March, 2022, pp. 4C11–4C16, https://doi.org/10.1109/IRPS48227.2022.9764572.

[22] M.J. Ellsworth, L.A. Campbell, R.E. Simons, M.K. Iyengar, R.R. Schmidt, R.C. Chu, The evolution of water cooling for IBM large server systems: back to the future, in: 2008 11th IEEE Intersociety Conference on Thermal and Thermomechanical Phenomena in Electronic Systems, I-THERM, 2008, pp. 266–274, https://doi.org/10.1109/ITHERM.2008.4544279.

[23] T. Gao, B.G. Sammakia, J. Geer, B. Murray, R. Tipton, R. Schmidt, Comparative analysis of different in row cooler management configurations in a hybrid cooling data center, in: ASME 2015 International Technical Conference and Exhibition on Packaging and Integration of Electronic and Photonic Microsystems, InterPACK 2015, Collocated with the ASME 2015 13th International Conference on Nanochannels, Microchannels, and Minichannels, vol. 1, Nov. 2015, https://doi.org/10.1115/IPACK2015-48069.

[24] U. Chowdhury, W. Hendrix, T. Craft, W. James, A. Sutaria, D. Agonafer, OptiCmal Design and Modeling of Server Cabinets with In-Row Coolers and Air Conditioning Units in a Modular Data Center, asmedigitalcollection.asme.org, 2019 [Online]. Available: https://asmedigitalcollection.asme.org/InterPACK/proceedings-abstract/InterPACK2019/V001T02A009/1071704?casa_token=g0Za9sKN9ucAAAAA:PgUSeqlPRDpyocqKdSYcYDiR2VnFVdUzK8Dipz4dYK8Yl_fe4Zb19YDUqew-eInQXmcHMw6KbA. (Accessed 15 April 2023).

[25] R. Schmidt, M. Iyengar, D. Porter, G. W.-2010 12th I., and undefined, Open Side Car Heat Exchanger that Removes Entire Server Heat Load without Any Added Fan Power, ieeexplore.ieee.org, 2010. https://ieeexplore.ieee.org/abstract/document/5501423/?casa_token=CCCi1PsOjVAAAAAA:at8SWiOd2YdZ_LOjxcIGiSkLi8Dbth8W8tNt87q1qIWLayYWCFtbFx2p6DWx4xBumL1mT_szdfo. (Accessed 28 June 2023).

[26] A. Heydari, et al., Liquid to air cooling for high heat density liquid cooled data centers, in: Proceedings of ASME 2022 International Technical Conference and Exhibition on Packaging and Integration of Electronic and Photonic Microsystems, InterPACK 2022, Dec. 2022, https://doi.org/10.1115/IPACK2022-97386.

[27] H. Coles, S. Greenberg, P. H.-D. C. Handbook, and undefined, Rack-level cooling and cold plate cooling. ndl.ethernet.edu.etH Coles, S Greenberg, P HughesData Center Handbook, 2014•ndl.ethernet.edu.et, 2014. http://ndl.ethernet.edu.et/bitstream/123456789/21494/1/6.pdf#page=513. (Accessed 6 December 2023).

[28] M.J. Ellsworth, G.F. Goth, R.J. Zoodsma, A. Arvelo, L.A. Campbell, W.J. Anderl, An overview of the IBM Power 775 supercomputer water cooling system, Journal of Electronic Packaging, Transactions of the ASME 134 (2) (2012), https://doi.org/10.1115/1.4006140.

[29] M. Iyengar, et al., Server liquid cooling with chiller-less data center design to enable significant energy savings. Annual IEEE Semiconductor Thermal Measurement and Management Symposium, 2012, pp. 212–223, https://doi.org/10.1109/STHERM.2012.6188851.

[30] S. Nada, R. El-Zoheiry, M. E.-C. S. in T., and undefined, Experimental Investigation of Hydrothermal Characteristics of Data Center Servers' Liquid Cooling System for Different Flow Configurations and Geometric, Elsevier, 2021. https://www.sciencedirect.com/science/article/pii/S2214157X21004391. (Accessed 28 June 2023).

[31] H. Chen, Y. hang Peng, Y. ling Wang, Thermodynamic analysis of hybrid cooling system integrated with waste heat reusing and peak load shifting for data center, Energy Convers. Manag. 183 (Mar. 2019) 427–439, https://doi.org/10.1016/J.ENCONMAN.2018.12.117.

[32] P. Shahi, S. Saini, P. B.-I. T. on, and undefined, A comparative study of energy savings in a liquid-cooled server by dynamic control of coolant flow rate at server level, ieeexplore.ieee.org, 2021. https://ieeexplore.ieee.org/abstract/document/9381248/?casa_token=EXMgRhyKF8QAAAAA:otSk-9uabaS9fj3LhCnyDE6vC1kLaW_4zo5WVPnkF7ElRVLh0pYLkuNOBdqIiOoVLktAkWnqdaQ. (Accessed 15 April 2023).

[33] Y.M. Manaserh, M.I. Tradat, A.R. Gharaibeh, B.G. Sammakia, R. Tipton, Shifting to energy efficient hybrid cooled data centers using novel embedded floor tiles heat exchangers, Energy Convers. Manag. 247 (Nov. 2021) 114762, https://doi.org/10.1016/J.ENCONMAN.2021.114762.

[34] L. Ling, Q. Zhang, Y. Yu, S. L.-A. T. Engineering, and undefined, Experimental Investigation on the Thermal Performance of Water Cooled Multi-Split Heat Pipe System (MSHPS) for Space Cooling in Modular Data Centers, Elsevier, 2016. https://www.sciencedirect.com/science/article/pii/S1359431116311358?casa_token=gt4NNlBRUpEAAAAA:ohY–4NdmfT5TkkP3sDswMig9gUIoCG-kIhMy4g40OgpUND2InMKURGqywVCbcstceesJ4DAV-B8. (Accessed 16 December 2023).

[35] P. Shahi, et al., Methodology to characterize row manifolds for high power direct to chip liquid cooling data centers. asmedigitalcollection.asme.orgP Shahi, A Heydari, B Eslami, V Radmard, C Hinge, H Modi, LSR Chinthaparthy, M TradatInternational Electronic Packaging Technical, 2023•asmedigitalcollection.asme.org, 2023 [Online]. Available: https://asmedigitalcollection.asme.org/InterPACK/proceedings-abstract/InterPACK2023/87516/1170947?casa_token=-K2slv2F51kAAAAA:63yzpULnHLxXJkFSoMC17CbhbpZFF6zh0SdeLTdWmKUam8ByNEcrHYMbct7ed3okekO8AJok3w. (Accessed 15 December 2023).

[36] A.H. Nvidia, et al., Experimental study of transient hydraulic characteristics for liquid cooled data center deployment. asmedigitalcollection.asme.orgA Heydari, P Shahi, V Radmard, B Eslami, U Chowdhury, A Sivakumar, A LakshminarayanaInternational Electronic Packaging Technical, 2022•asmedigitalcollection.asme.org, 2022 [Online]. Available: https://asmedigitalcollection.asme.org/InterPACK/proceedings-abstract/InterPACK2022/V001T01A009/1153374?casa_token=4jBtdK7iGTYAAAAA:04D7iOC24jU2L0B8fTu1eVPzzmOSf5xEOR9wit4suua6m8ZrCaDLILDox7Nugo9bNsnSMFzk6Q. (Accessed 15 December 2023).

[37] A. Heydari, et al., Guidelines and experimental hydraulic performance evaluation for single-phase CDUs under steady and transient events. InterSociety Conference on Thermal and Thermomechanical Phenomena in Electronic Systems, ITHERM, 2023-May, 2023, https://doi.org/10.1109/ITHERM55368.2023.10177633.

[38] A. Heydari, Q. Soud, M. T.-2023 22nd I., and undefined, An investigation of multi-parameters effects on the performance of liquid-to-liquid heat exchangers in rack level cooling. ieeexplore.ieee.orgA Heydari, Q Soud, M Tradat, A Gharaibeh, N Fallahtafti, P Shahi, J Rodriguez, B Sammakia2023 22nd IEEE Intersociety Conference on Thermal and, 2023•ieeexplore.ieee.org, 2023. https://ieeexplore.ieee.org/abstract/document/10177525/?casa_token=rJB11WWOsV0AAAAA:hdVg8z0NmwcKi5Th_dRqWGhLFb3cOG3EYnHhKJ5u2TlOYIivgtuEq-IiV0D7jcQiGioWEMrbYGE. (Accessed 16 December 2023).

[39] A. Heydari, et al., L2A CDUs performance and considerations for server rooms upgrade with conventional air conditioning. asmedigitalcollection.asme.orgA Heydari, Q Soud, M Tradat, A Gharaibeh, N Fallahtafti, J Rodriguez, B SammakiaInternational Electronic Packaging Technical, 2023•asmedigitalcollection.asme.org, 2023, in: https://asmedigitalcollection.asme.org/InterPACK/proceedings-abstract/InterPACK2023/87516/1170981?casa_token=rkc5oSkEcEUAAAAA:Tz2PmOjyWISCCwnUaDPcSVe7694E0OvutGxrq-TMEi1Mq44dQtmo96jXqQgL04_yx6x8mvVYMg. (Accessed 16 December 2023).

[40] A. Heydari, et al., Performance analysis of liquid-to-air heat exchanger of high-power density racks, J. Electron. Packag. 146 (4) (Dec. 2024), https://doi.org/10.1115/1.4065537.

[41] A. Heydari, A. Gharaibeh, M. Tradat, Y. M.-A. T., and undefined, Experimental Evaluation of Direct-To-Chip Cold Plate Liquid Cooling for High-Heat-Density Data Centers, Elsevier, 2023. https://www.sciencedirect.com/science/article/pii/S1359431123021518. (Accessed 16 December 2023).

[42] A. Heydari, et al., At scale development of thermal test vehicles for data center liquid cooling developments. asmedigitalcollection.asme.orgA Heydari, H Miyamura, U Chowdhury, YMA Manaserh, M Tradat, P Shahi, V RadmardInternational Electronic Packaging Technical, 2023•asmedigitalcollection.asme.org, 2023 [Online]. Available: https://asmedigitalcollection.asme.org/InterPACK/proceedings-abstract/InterPACK2023/87516/1170937?casa_token=Vj3qtWFTLxIAAAAA:vrrAkWVNO49XCtXKBICigKpcBgpkFJFZgJ2_m4pMw8ek-8kREEHnqi7bZmlty_ZMpsbuZsV03A. (Accessed 6 December 2023).

[43] "Data Center Power Equipment Thermal Guidelines and... - Google Scholar." Accessed: Apr. 14, 2023. [Online]. Available: http://tc0909.ashraetcs.org/documents/ASHRAE_TC0909_Power_White_Paper_22_June_2016_REVISED.pdf [Accessed: 15-July- 2019].

[44] A. Isazadeh, D. Ziviani, D.E. Claridge, Thermal management in legacy air-cooled data centers: an overview and perspectives, Renew. Sustain. Energy Rev. 187 (Nov. 2023) 113707, https://doi.org/10.1016/J.RSER.2023.113707.

[45] A. Velte-Schäfer, C. Teicht, M. Stahlhut, T. M.-E. C. and, and undefined, Utilizing waste heat from data centers with adsorptive heat transformation–Heat exchanger design and choice of adsorbent. ElsevierA Velte-Schäfer, C Teicht, M Stahlhut, T May, R Herrmann, T Urbaneck, G FüldnerEnergy Conversion and Management, 2024•Elsevier, 2024. https://www.sciencedirect.com/science/article/pii/S0196890424004412. (Accessed 5 June 2024).

[46] S. Pourahmad, S.M. Pesteei, Effectiveness-NTU analyses in a double tube heat exchanger equipped with wavy strip considering various angles, Energy Convers. Manag. 123 (Sep. 2016) 462–469, https://doi.org/10.1016/J.ENCONMAN.2016.06.063.

[47] K. Jin, A.B. Krishna, Z. Wong, P.S. Ayyaswamy, I. Catton, T.S. Fisher, Thermohydraulic experiments on a supercritical carbon dioxide–air microtube heat exchanger, Int. J. Heat Mass Tran. 203 (Apr. 2023) 123840, https://doi.org/10.1016/J.IJHEATMASSTRANSFER.2022.123840.

[48] M. Seddiq, M. M.-I, J. of H. and M. Transfer, and undefined, Analytical solution for heat transfer problem in a cross-flow plate heat exchanger. ElsevierM Seddiq, M MaerefatInternational Journal of Heat and Mass Transfer, 2020•Elsevier, 2020. https://www.sciencedirect.com/science/article/pii/S0017931020333469. (Accessed 9 June 2024).
[49] A.P. Wemhoff, A. Ortega, An exergy-based analysis of the effects of rear door heat exchange systems on data center energy efficiency, in: Thermomechanical Phenomena in Electronic Systems -Proceedings of the Intersociety Conference, Sep. 2014, pp. 1129–1136, https://doi.org/10.1109/ITHERM.2014.6892407.
[50] R. Khosravi, A. Khosravi, S. Nahavandi, H. Hajabdollahi, Effectiveness of evolutionary algorithms for optimization of heat exchangers, Energy Convers. Manag. 89 (Jan. 2015) 281–288, https://doi.org/10.1016/J.ENCONMAN.2014.09.039.
[51] M. Hnayno, A. Chehade, H. Klaba, H. B.-A. T., and undefined, Performance analysis of new liquid cooling topology and its impact on data centres. ElsevierM Hnayno, A Chehade, H Klaba, H Bauduin, G Polidori, C MaaloufApplied Thermal Engineering, 2022•Elsevier, 2022. https://www.sciencedirect.com/science/article/pii/S1359431122006779. (Accessed 3 June 2024).
[52] C. Jiang, Y. Qi, J. Li, X. Mei, W. Li, E. Shi, Stochastic simulation of magnetically controlled convection in porous media with random porosity via Karhunen-Loève expansion and intrusive polynomial chaos expansion, Int. J. Heat Mass Tran. 224 (Jun. 2024) 125387, https://doi.org/10.1016/J.IJHEATMASSTRANSFER.2024.125387.